ARTICLE

Tuning Magnetism in Zigzag ZnO Nanoribbons by Transverse Electric Fields

Liangzhi Kou,[†] Chun Li,[‡] Zhuhua Zhang,[†] and Wanlin Guo[†,*]

[†]Institute of Nano Science, Nanjing University of Aeronautics and Astronautics, Nanjing 210016, China, and [‡]School of Mechanics, Civil Engineering and Architecture, Northwestern Polytechnical University, Xi'an 710072, China

ABSTRACT We show by first-principles calculations that the magnetic moments of zigzag ZnO nanoribbons can be efficiently modulated by transverse electric fields. Depending on the field direction, the total magnetic moment in a zigzag ZnO nanoribbon can be remarkably enhanced or reduced and even completely quenched with increasing field over a threshold strength. However, in weak electric fields below the threshold, the magnetic moment in the zigzag ZnO nanoribbons nearly remains unchanged, which can be explained in terms of intrinsic transverse electric polarization and quantum confinement effects. The threshold electric field required to modulate the magnetic moment decreases significantly with increasing ribbon width, showing practical importance.

KEYWORDS: tunable magnetism · ZnO nanoribbon · electric field · first-principles calculation

Control of magnetization is central to magnetic storage technology as well as spin-polarized transport. Currently, the magnetism in various types of memory elements is manipulated through magnetic field, which, however, has great handicaps of low storage density and high writing energy.[1] In contrast, electrical control of magnetization allows lower energy consumption and promises a device conception fully compatible with existing microelectronic technology.[2−5] Present electrical manipulation of magnetism is usually reported in multiferroic metal oxides and films;[6−8] however, the complicated interface heterostructures necessary for the coupling of the order parameters make such kinds of materials uncommon and still limited to basic demonstration devices. Therefore, achieving electrical control of magnetization in simple and commonly used materials represents a promising field for practical applications. As a typical wide band gap and piezoelectric semiconductor, ZnO and its related nanostructures have attracted considerable attention in both scientific research and technological applications.[9−11] In particular, although magnetism in ZnO nanoribbons (ZNNRs) has not been clearly observed in experiment, to the best of our knowledge, planar zigzag ZnO nanoribbons (Z-ZNNRs) have been predicted to possess substantial magnetism along the O-terminated edge and hold great promise for implementation in spintronic devices.[12,13] Moreover, ZNNRs have been synthesized[14] and successfully used as building blocks in many nanodevices, such as field effect transistors,[9] ultrasensitive nanosize gas sensors,[15] nanoresonators,[11] nanocantilevers,[16] and so on, owing to their excellent optical, piezoelectric, and biocompatible properties inherited from the bulk material.[17,18] Therefore, there is strong motivation to examine whether the electrical control of magnetization can be realized in such emerging structures. In this work, we report a first-principles study on magnetism modulation in ferromagnetic zigzag ZnO nanoribbons by transversely applied electric fields. We show that the electric field can significantly enhance or reduce the edge magnetism of Z-ZNNRs by adjusting its magnitude and direction. Especially, the required electric field strength to change the magnetic moment decreases remarkably with increasing width of the Z-ZNNRs. Similar modulation of magnetism is also found in stacked trilayer Z-ZNNRs. The predicted electrically controllable magnetism has potential applications in magnetic switch and data storage.

RESULTS AND DISCUSSION

The ground state of a monolayer Z_5-ZNNR (refer to Methods) with a width of 1.14 nm is calculated to be ferromagnetic metal with a magnetic moment of 0.986 μ_B/supercell, which is consistent with the previous calculated results.[12,19] This ferromagnetism is stable even at room temperature since predicted total energy of the ferromagnetic state is 0.155 eV lower than that

*Address correspondence to wlguo@nuaa.edu.cn.

Received for review November 4, 2009 and accepted March 8, 2010.

Published online March 16, 2010. 10.1021/nn901552b

© 2010 American Chemical Society

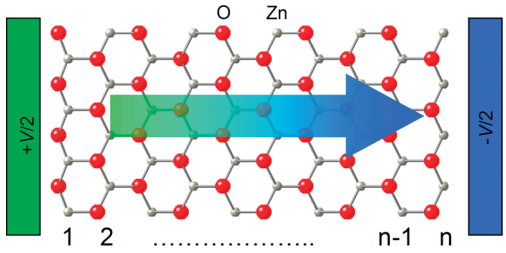

Figure 1. Schematic diagram of a Z-ZNNR under a transversely applied electric field. The positive electric field is illustrated by the broad arrow pointing from the O-terminated edge to the Zn-terminated edge. The Z-ZNNR is infinitely long along the vertical direction. Two armchair chains along the width direction are chosen for supercells calculated in this work.

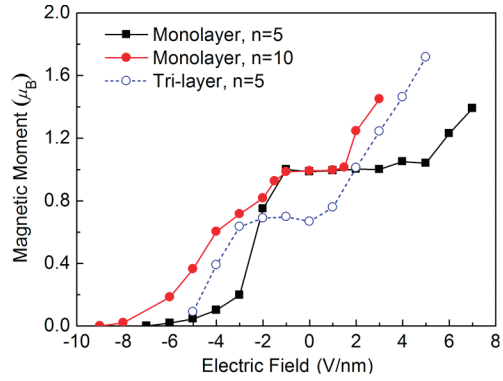

Figure 2. Magnetic moments per supercell of different Z-ZNNRs as a function of applied electric fields.

of the antiferromagnetic state. Interestingly, the magnetism can be modulated when a transverse electric field is applied across the width direction, as indicated in Figure 1. As shown in Figure 2, the asymmetrical nature of the Z-ZNNRs results in a field-induced nonlinear modulation on the magnetic moment. Particularly, a platform occurs in the region of low field strength for each studied nanoribbon. Here, we define the positive direction of an external field as pointing from the O-terminated edge to the Zn-terminated edge. For the Z_5-ZNNR under a positive field below 5 V/nm, the magnetic moment of the system is almost unchanged. A similar phenomenon is also observed in the case of negative electric field when the field strength is below 1 V/nm. In the following, we will call these critical values the positive and negative threshold electric fields, respectively.

However, the origins of the two threshold electric fields are distinctly different. Due to the positive and negative ionic charges at the Zn- and O-terminated edges, a spontaneous polarization exists across the Z-ZNNRs in the direction opposite to the positive field.[20] Thus, the magnetic moment of Z-ZNNRs can only be increased by a positive field large enough to overcome the intrinsic electric polarization. As the width increases, the positive threshold field will decrease drastically, as shown in Figure 2, for the Z_5- and Z_{10}-ZNNR. The reason is that the intrinsic polarization field E, which is proportional to the effective polarization line charge density, is reversely proportional to the ribbon width.[21] This is further corroborated by our calculations that the electrostatic potential difference ΔU between the two polarized edges slightly increases with increasing width (refer to Figure S1 in Supporting Information). So the equivalent intrinsic electric field, $E_{eq} = \Delta U/ew$, decreases with increasing ribbon width w. On the other hand, the negative threshold field to a great extent originates from the quantum confinement effects existing in such low-dimensional structures, where it is difficult for electrons to be driven by a low field strength,[10] leading to almost unchanged magnetic moments with electric fields. This confinement effect is not as profound as that of the internal polarization effect, thus the negative threshold field is relatively lower. It can be predicted that the quantum confinement effect of the nanoribbons becomes weaker in wider Z-ZNNRs, thus the negative threshold field will eventually disappear. As the actual ribbon widths usually reach up to tens or even hundreds of nanometers, the threshold field will be negligible therein, and the ribbon's magnetic moment will become sensitive to the applied electric fields. The insensitivity of magnetism against weak electric fields in narrow Z-ZNNRs may provide an opportunity to obtain robust ferromagnetism against perturbation from possible external fields.

Further increase in field strength beyond the threshold values will result in a remarkable modulation in the magnetic moment of the ribbon system. For the Z_5-ZNNR under a positive field above 5 V/nm, the external electric field leads to electron transfer from the Zn-terminated edge to the O-terminated edge (not shown here). Thus, more unpaired electrons accumulate at the O-terminated edge, resulting in the enhancement of magnetic moment, as illustrated by the maps of spatial magnetization density distributions (defined as the spin-up density mi-

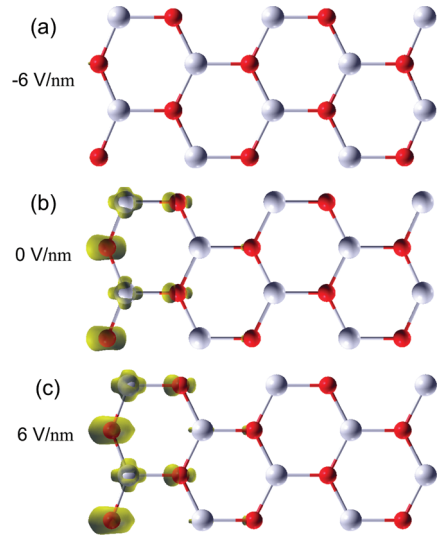

Figure 3. Spatial magnetization density distributions (up−down) in a Z_5-ZNNR under electric fields of (a) −6, (b) 0, and (c) 6 V/nm. The isosurface is uniformly set to be 0.01 e/Å^3.

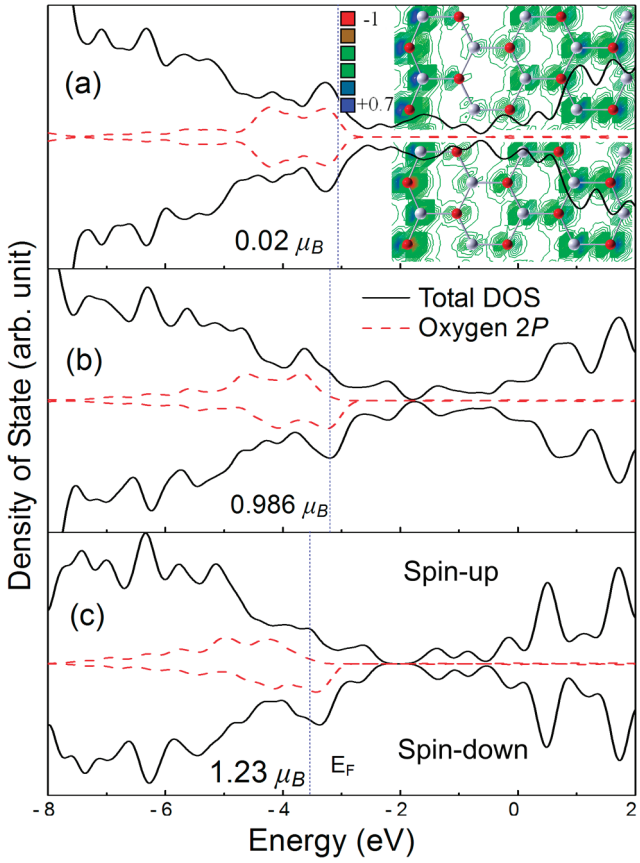

Figure 4. Spin-polarized total density of states (black solid lines) and partial density of states of the O 2p states (PDOS) at the O-terminated edge (red dashed lines) under electric fields of (a) −6, (b) 0, and (c) 6 V/nm. The blue dotted lines denote the Fermi level. Corresponding magnetic moment is listed for each case. Inset in (a) presents the field-induced spin density transfer [$\Delta\sigma = \sigma(E) - \sigma(0)$] for spin-up and spin-down electrons under the field strength of −6 V/nm. The scale bar is 10^{-1} $|e|$Å^{-2}.

nus the spin-down density) in Figure 3c. In contrast, with the reversed electric field beyond the negative threshold value applied, electrons transfer from the O-terminated edge to the Zn-terminated edge and the magnetic moment of the system decreases (see Figure 3a). With further increasing negative field to 7 V/nm, all of the electrons localized on the O-terminated edge are paired due to complete spin compensation (see detailed analysis below), giving rise to the system a nonmagnetic ground state. In particular, one can observe from Figure 2 that, for the wider Z_{10}-ZNNR, it requires a stronger negative electric field to quench the magnetism because more unpaired electrons are localized on the O-terminated edge. Besides the effect of electron transfers, the ionic effect on the magnetism modulation is investigated by fixing the positions of all atoms, which shows that the variation in magnetic moment of the system *via* electric field is nearly unchanged. Therefore, the ionic effect can be negligible in the magnetism modulation. The field-induced magnetism quench behavior has potential application in spintronic devices, such as a magnetic switch.

To understand the origin of this magnetism modulation behavior, the partial density of state (PDOS) of the edge oxygen atoms and the total DOS of Z_5-ZNNR are shown in Figure 4. From the DOS, one can observe that the states at the Fermi level (E_F) mostly come from the 2p orbitals of the edge O atoms, which exhibit asymmetrical spin state densities, as shown in Figure 4b. This is consistent with the fact that the unpaired electrons are mainly localized on the O-terminated edge of Z-ZNNRs[12] and, meanwhile, proves that it has different electron density distributions for spin-up and spin-down states on the edge. When a positive (negative) external electric field is applied, the electrostatic potential is lowered (raised) on the O-terminated edge. Correspondingly, the energies of edge O 2p states are shifted downward (upward). However, due to the different spin electron distributions on the O edge (Figure 5), the field-induced energy shifts of the spin-up and spin-down states are much different.[22] Under a negative field, the spin-up states at the O-terminated edge shift upward significantly while the upward shift of spin-down states is relatively smaller, leading to a decrease of spin polarization at E_F (Figure 6). This process reduces the magnetic moment at the O-terminated edge. The spin-dependent electron screening effect is also evidenced in the field-induced spin electron transfer, as illustrated in the inset of Figure 4a, where a more remarkable accumulation of spin-up electrons is observed at the O-terminated edge than that of spin-down electrons. With further increasing negative field strength, the DOS for spin-up and spin-down states eventually become equal at E_F due to the complete spin compensation, consequently leading to a nonmagnetic ribbon. A contrary behavior is observed under a positive electric field (Figure 4c), which results in a rapid downshift of the spin-up states and an increase in the spin polarization at E_F, thus significantly enhances the magnetic moment of the system.

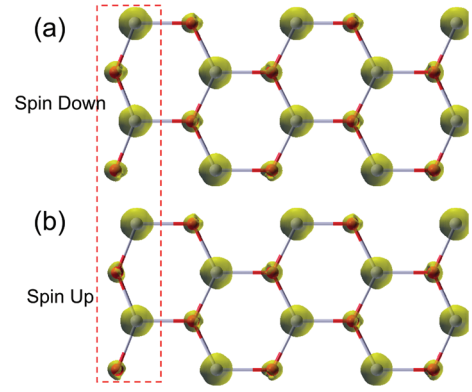

Figure 5. Charge distributions for the spin-down state (a) and spin-up state (b) of the Z_5-ZNNR under zero field. The isosurface is 0.4 e/Å^3. Note that the charge density of different spin states is obviously different on the O-terminated edge, especially on the edge O atoms, as indicated by the red dashed rectangle, and can also be reflected by the magnetization density distribution localized on the edge, as shown in Figure 3b.

When a second layer is stacked on top of the monolayer, the system becomes a nonmagnetic semiconductor[17] and hence is beyond the scope of our discussions. However, the metallic magnetic ground state is recovered when a third layer is additionally stacked on the system, with a slightly reduced magnetic moment compared to that in monolayer ribbon due to interlayer interaction. The corresponding magnetism modulation for the trilayer Z_5-ZNNR is also shown in Figure 2. In this case, the field-induced magnetism modulation exhibits some differences from the case of the monolayer ribbon with the same width. The positive threshold electric field is remarkably reduced owing to the reduction of the interior ionic potential difference induced by the interaction of edge atoms at different layers. Instead, the interaction makes electrons more strongly confined to their original edges and thus more difficult to be moved. Therefore, a stronger negative threshold electric field is required to reduce the magnetic moment of the trilayer system in comparison with the monolayer system with the same width.

The presence of substrate may significantly affect the magnetism of Z-ZNNRs, which in turn changes the magnetism modulation. So it is necessary to clarify the effect of substrate on the magnetism and its modulation for practical applications. In fact, for the ZNNRs on some inactive substrates, such as SiO_2, there should be only a physical interaction and the magnetism modulation can be survived;[23] whereas for active surfaces, such as Si(001) surface, the first single-layer ZNNR on the substrate will act as a buffer layer due to the chemical bonding between them, and the magnetism modulation will reappear in the second ribbon layer on the system.[24,25] This discussion indicates the possibility of designing magnetic devices settled on essential substrates. Of course, the stability of the magnetic edge state on the substrate at finite temperature is an important issue for further research.

CONCLUSION

In conclusion, our first-principles calculations show that the magnetic properties of Z-ZNNRs can be modulated by transversely applied external electric fields over a threshold value. When the field strength is below the threshold value, the magnetic moment of a Z-ZNNR is nearly unchanged. Above the threshold field, the magnetic moment of the system is significantly enhanced by a positive field while rapidly reduced and even eventually quenched under a negative field. Further analysis shows that the positive and negative threshold fields are mainly derived from intrinsic transverse electric polarization and quantum confinement effects, respectively. As the threshold field strength decreases with increasing ribbon width, such electric field modulated spin polarization has practical importance for novel spintronics applications. The present theoretical results may encourage experimentalists to search for the external field sensitivity of magnetic properties in ZNNRs and similar nanostructures in the near future.

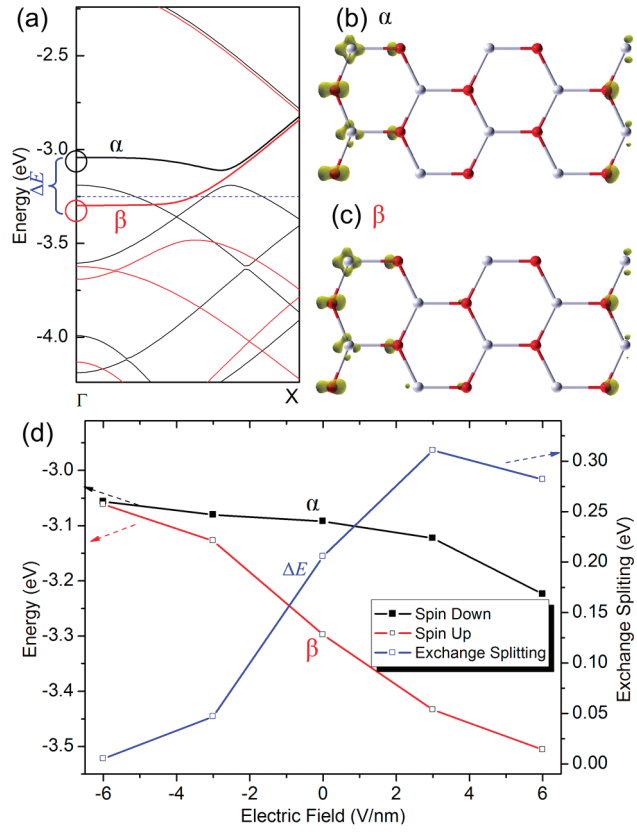

Figure 6. (a) Spin-polarized band structure of the Z_5-ZNNR under zero field (down, black; up, red). The denoted spin-down state (α) and spin-up state (β) are split from the same spin-unpolarized band; the energy interval between them at Γ point is denoted as Δ*E* (the exchange splitting). The spin charge distributions of α (b) and β (c) at Γ point are shown when no electric field is applied [0.005 *e*/Å^3]. (d) Energy shifts of the spin band α (black line) and β (red line) at Γ point as a function of applied electric field, together with the variation of the exchange splitting (blue line).

METHODS

Our calculations are performed using the SIESTA package[26] with the local spin density approximation (LSDA)[27] for the exchange correlation function. The double-ζ polarized numerical atomic orbital basis sets for Zn and O are used. All atoms are allowed to relax under applied external electric field until the force on each atom is less than 0.02 eV/Å. The Brillouin integration is sampled with 2 × 2 × 6 Monkhorst meshes. An equivalent plane wave cutoff of 250 hartree is chosen in the simulations. Vacuum layers of at least 10 Å are chosen in width and thickness directions. All of these parameters have been successfully used in our previous works on ZnO nanostructures,[28,29] thus ensuring their validity. The external electric field is modeled by transversely adding a sawtoothlike potential to the nanoribbons.[30]

The Z-ZNNRs in our studies are originally constructed by cutting a planar monolayer along zigzag lines, as shown in Figure 1. For the structure with a few ZnO layers, it has been recently demonstrated that each layer prefers a planar configuration in

which both cations and anions are coplanar after relaxation.[31,32] The multilayer ribbons are constructed by placing the planar layers on top of each other with AB stacking. For convenience, the Z-ZNNRs are classified by the number of zigzag chains (n) across the ribbon width and denoted as Z_n-ZNNR.

Acknowledgment. This work is supported by the 973 Program (No.2007CB936204), National NSF (No. 10732040), Jiangsu Province NSF (BK2008042), and the Ministry of Education (No.705021, IRT0534) of China. C.L. acknowledges support from the Fundamental Research Fund (No. JC200935) and the Ao-Xiang Star Project of Northwestern Polytechnical University.

Supporting Information Available: Electrostatic potential differences along the width direction of Z_5- and Z_{10}-ZNNR are calculated. This material is available free of charge *via* the Internet at http://pubs.acs.org.

REFERENCES AND NOTES

1. Chiba, D.; Yamanouchi, M.; Matsukura, F.; Ohno, H. Electrical Manipulation of Magnetization Reversal in a Ferromagnetic Semiconductor. *Science* **2003**, *301*, 943–945.
2. Ohno, H.; Chiba, D.; Matsukura, F.; Omiya, T.; Abe, E.; Dietl, T.; Ohno, Y.; Ohtani, K. Electric-Field Control of Ferromagnetism. *Nature* **2000**, *408*, 944–946.
3. Lottermoser, T.; Lonkai, T.; Amann, U.; Hohlwein, D.; Ihringer, J.; Fiebig, M. Magnetic Phase Control by an Electric Field. *Nature* **2004**, *430*, 541–544.
4. Chiba, D.; Sawicki, M.; Nishitani, Y.; Nakatani, Y.; Matsukura, F.; Ohno, H. Magnetization Vector Manipulation by Electric Fields. *Nature* **2008**, *455*, 515–518.
5. Zhao, T.; Scholl, A.; Zavaliche, F.; Lee, K.; Barry, M.; Doran, A.; Cruz, M. P.; Chu, Y. H.; Ederer, C.; Spaldin, N. A.; *et al.* Electrical Control of Antiferromagnetic Domains in Multiferroic $BiFeO_3$ Films at Room Temperature. *Nat. Mater.* **2006**, *5*, 823–829.
6. Duan, C.-G.; Jaswal, S. S.; Tsymbal, E. Y. Predicted Magnetoelectric Effect in Fe/$BaTiO_3$ Multilayers: Ferroelectric Control of Magnetism. *Phys. Rev. Lett.* **2006**, *97*, 047201.
7. Duan, C.-G.; Velev, J. P.; Sabirianov, R. F.; Zhu, Z.; Chu, J.; Jaswal, S. S.; Tsymbal, E. Y. Surface Magnetoelectric Effect in Ferromagnetic Metal Films. *Phys. Rev. Lett.* **2008**, *101*, 137201.
8. Zavaliche, F.; Zhao, T.; Zheng, H.; Straub, F.; Cruz, M. P.; Yang, P.-L.; Hao, D.; Ramesh, R. Electrically Assisted Magnetic Recording in Multiferroic Nanostructures. *Nano Lett.* **2007**, *7*, 1586–1590.
9. Cha, S. N.; Jang, J. E.; Choi, Y.; Amaratunga, G. A. J.; Ho, G. W.; Welland, M. E.; Hasko, D. G.; Kang, D. J.; Kim, J. M. High Performance ZnO Nanowire Field Effect Transistor Using Self-Aligned Nanogap Gate Electrodes. *Appl. Phys. Lett.* **2006**, *89*, 263102.
10. Li, C.; Guo, W.; Kong, Y.; Gao, H. Size-Dependent Piezoelectricity in Zinc Oxide Nanofilms from First-Principles Calculations. *Appl. Phys. Lett.* **2007**, *90*, 033108.
11. Bai, X. D.; Gao, P. X.; Wang, Z. L.; Wang, E. G. Dual-Mode Mechanical Resonance of Individual ZnO Nanobelts. *Appl. Phys. Lett.* **2003**, *82*, 4806.
12. Botello-Méndez, A. R.; López-Urías, F.; Terrones, M.; Terrones, H. Magnetic Behavior in Zinc Oxide Zigzag Nanoribbons. *Nano Lett.* **2008**, *8*, 1562–1565.
13. Botello-Méndez, A. R.; López-Urías, F.; Terrones, M.; Terrones, H. Enhanced Ferromagnetism in ZnO Nanoribbons and Clusters Passivated with Sulfur. *Nano Res.* **2008**, *1*, 420–426.
14. Pan, Z. W.; Dai, Z. R.; Wang, Z. L. Nanobelts of Semiconducting Oxides. *Science* **2001**, *291*, 1947–1949.
15. Comini, E.; Faglia, G.; Sberveglieri, G.; Pan, Z. W.; Wang, Z. L. Stable and Highly Sensitive Gas Sensors Based on Semiconducting Oxide Nanobelts. *Appl. Phys. Lett.* **2002**, *81*, 1869.
16. Hughes, W.; Wang, Z. L. Nanobelts as Nanocantilevers. *Appl. Phys. Lett.* **2003**, *82*, 2886.
17. Zhao, M. H.; Wang, Z. L.; Mao, S. X. Piezoelectric Characterization of Individual Zinc Oxide Nanobelt Probed by Piezoresponse Force Microscope. *Nano Lett.* **2004**, *4*, 587–590.
18. Özgür, Ü.; Alivov, Y. I.; Liu, C.; Teke, A.; Reshchikov, M. A.; Doğan, S.; Avrutin, V.; Cho, S.-J.; Morkoc, H. A Comprehensive Review of ZnO Materials and Devices. *J. Appl. Phys.* **2005**, *98*, 041301.
19. Botello-Méndez, A. R.; Martínez-Martínez, M. T.; López-Urías, F.; Terrones, M.; Terrones, H. Metallic Edges in Zinc Oxide Nanoribbons. *Chem. Phys. Lett.* **2007**, *448*, 258–263.
20. Kong, X. Y.; Wang, Z. L. Spontaneous Polarization-Induced Nanohelixes, Nanosprings, and Nanorings of Piezoelectric Nanobelts. *Nano Lett.* **2003**, *3*, 1625–1631.
21. Park, C. H.; Louie, S. G. Energy Gaps and Stark Effect in Boron Nitride Nanoribbons. *Nano Lett.* **2008**, *8*, 2200–2203.
22. Son, Y.; Cohen, M. L.; Louie, S. G. Half-Metallic Graphene Nanoribbons. *Nature* **2006**, *444*, 347–349.
23. Ishigami, M.; Chen, J. H.; Cullen, W. G.; Fuhrer, M. S.; Williams, E. D. Atomic Structure of Graphene on SiO_2. *Nano Lett.* **2007**, *7*, 1643–1648.
24. Zhang, Z.; Guo, W. Electronic Properties of Zigzag Graphene Nanoribbons on Si(001). *Appl. Phys. Lett.* **2009**, *95*, 023107.
25. Zhang, Z.; Chen, C.; Guo, W. Magnetoelectric Effect in Graphene Nanoribbons on Substrates *via* Electric Bias Control of Exchange Splitting. *Phys. Rev. Lett.* **2009**, *103*, 187204.
26. Soler, J. M.; Artacho, E.; Gale, J. D.; García, A.; Junquera, J.; Ordejón, P.; Sánchez-Portal, D. The SIESTA Method for *Ab Initio* Order-N Materials Simulation. *J. Phys.: Condens. Matter* **2002**, *14*, 2745–2779.
27. Ceperley, D. M.; Alder, B. J. Ground State of the Electron Gas by a Stochastic Method. *Phys. Rev. Lett.* **1980**, *45*, 566.
28. Li, C.; Guo, W.; Kong, Y.; Gao, H. First-Principles Study on ZnO Nanoclusters with Hexagonal Prism Structures. *Appl. Phys. Lett.* **2007**, *90*, 223102.
29. Li, C.; Guo, W.; Kong, Y.; Gao, H. First-Principles Study of the Dependence of Ground-State Structural Properties on the Dimensionality and Size of ZnO Nanostructures. *Phys. Rev. B* **2007**, *76*, 035322.
30. According to the theory used in the SIESTA code, the potential generated by an external electric field in z (nonbulk) directions is modeled as a term $V(z) = |e|E \cdot z(-w/2 < z \leq w/2)$, where E is the magnitude of the applied electric field and w is the size of the supercell.
31. Claeyssens, F.; Freeman, C. L.; Allan, N. L.; Sun, Y.; Ashfold, M. N. R.; Harding, J. H. Growth of ZnO Thin Films—Experiment and Theory. *J. Mater. Chem.* **2005**, *15*, 139–148.
32. Tusche, C.; Meyerheim, H. L.; Kirschner, J. Observation of Depolarized ZnO(0001) Monolayers: Formation of Unreconstructed Planar Sheets. *Phys. Rev. Lett.* **2007**, *99*, 026102.